

# Tuning of electron transport through a moebius strip: shot noise

Santanu K. Maiti<sup>1,2,\*</sup>

<sup>1</sup>*Theoretical Condensed Matter Physics Division, Saha Institute of Nuclear Physics,  
1/AF, Bidhannagar, Kolkata-700 064, India*

<sup>2</sup>*Department of Physics, Narasinha Dutt College, 129, Belilious Road, Howrah-711 101, India*

## Abstract

We explore electron transport through a moebius strip attached to two metallic electrodes by the use of Green's function technique. A parametric approach is used based on the tight-binding model to characterize the electron transport through such a bridge system and it is observed that the transport properties are significantly affected by (a) the transverse hopping strength between the two channels and (b) the strip-to-electrode coupling strength. In this context we also describe the noise power of the current fluctuations that provides a key information about the electron correlation which is obtained by calculating the Fano factor ( $F$ ). The knowledge of this current fluctuations gives important ideas for fabrication of efficient electronic devices.

**PACS No.:** 73.23.-b; 73.63.Rt; 73.40.Jn; 85.65.+h

**Keywords:** Moebius strip; Transverse hopping; Conductance;  $I$ - $V$  characteristic and Shot noise.

\*Corresponding Author: Santanu K. Maiti  
Electronic mail: santanu.maiti@saha.ac.in

# 1 Introduction

The advancements in nanoscience and technologies prompting a growing number of researchers across multiple disciplines to attempt to devise innovative ways for decreasing the size and increasing the performance of microelectronic circuits. One possible route is based on the idea of using molecules and molecular structures as functional devices. Following experimental developments, theory can play a major role in understanding the new mechanisms of conductance, but, the goal of developing a reliable molecular-electronics technology is still over the horizon and many key problems, such as device stability, reproducibility and the control of single-molecule transport need to be solved. Quantum transport properties through molecules was first studied theoretically during 1970's [1]. Later several experiments [2, 3, 4, 5, 6] have been carried out on electron transport through molecules placed between two metallic electrodes with few nanometer separation. It is very essential to control electron conduction through such quantum devices and the present understanding about it is quite limited. For example, it is not so clear how the molecular transport is affected by the structure of the molecule itself or by the nature of its coupling to the electrodes [7]. The electron conduction through such two-terminal devices can be controlled by some bias or gate voltage across the device. The current passing across the junction then becomes a strongly non-linear function of the applied voltage, and its understanding is a highly challenging problem. The knowledge of current fluctuations (quantum origin) provides a key idea for fabrication of efficient molecular devices. Blanter *et al.* [8] have described elaborately how the lowest possible noise power of the current fluctuations can be determined in a two-terminal conductor. The steady state current fluctuations, the so-called shot noise, is a consequence of the quantization of charge and it can be used to obtain information on a system which is not available through conductance measurements. The noise power of the current fluctuations provides an additional important information about the electron correlation by calculating the Fano factor ( $F$ ) which directly informs us whether the magnitude of the shot noise achieves the Poisson limit ( $F = 1$ ) or the sub-Poisson ( $F < 1$ ) limit.

In a recent experiment Tanda *et al.* [9] have fabricated a microscopic NbSe<sub>3</sub> moebius strip and it raises some interesting questions regarding the topological effect on quantum transport. In some

theoretical papers [10, 11] the topological effect on quantum transport for isolated moebius strips has been described and it has been observed that the transverse hopping strength has significant role on such transport. For non-zero transverse hopping strength, a moebius strip becomes a regular two-channel ring. On the other hand, when electrons are unable to move along the transverse direction a moebius strip reduces to a single-channel ring with doubling its length than the previous one. This is due to the peculiar topology of a moebius strip. In the present article we are interested about the electron transport properties through such a moebius strip which is attached to two metallic electrodes. Here we address a simple analytical formulation of the transport problem through the moebius strip using the tight-binding Hamiltonian. There exist some *ab initio* methods for the calculation of conductance [12, 13, 14, 15, 16, 17, 18, 19] as well as model calculations [20, 21, 22, 23, 24, 25, 26, 27, 28]. The model calculations are motivated by the fact that the *ab initio* methods are computationally too expensive and also provide a better insight to the problem and here we concentrate only on the qualitative results rather than the quantitative ones.

The plan of the paper is as follows. Section 2 describes the methodology for the calculation of electron transport through a finite size conductor sandwiched between two metallic electrodes. In Section 3, we study the conductance ( $g$ ) behavior as a function of energy ( $E$ ), the current ( $I$ ) and the noise power ( $S$ ) of its fluctuations as a function of applied bias voltage ( $V$ ) for some typical moebius strips. Finally, we summarize our results in Section 4.

## 2 Theoretical formulation

Here we formulate the technique for the calculation of transmission probability ( $T$ ), conductance ( $g$ ), current ( $I$ ) and noise power of current fluctuations ( $S$ ) for a finite size conductor attached with two metallic electrodes (schematically represented in Fig. 1) by the use of Green's function technique.

At low temperatures and bias voltage the conductance  $g$  of the conductor is given by the Landauer conductance formula [29],

$$g = \frac{2e^2}{h} T \quad (1)$$

where the transmission probability  $T$  becomes [29],

$$T = \text{Tr} [\Gamma_S G_C^r \Gamma_D G_C^a] \quad (2)$$

where  $G_C^r$  ( $G_C^a$ ) is the retarded (advanced) Green's function of the conductor and  $\Gamma_S$  ( $\Gamma_D$ ) describes its coupling to the source (drain). The Green's function of the conductor is expressed as,

$$G_C = (E - H_C - \Sigma_S - \Sigma_D)^{-1} \quad (3)$$

where  $E$  is the energy of the injecting electron and  $H_C$  is the Hamiltonian of the conductor which can be expressed in the tight-binding model within the non-interacting picture as,

$$H_C = \sum_i \epsilon_i c_i^\dagger c_i + \sum_{\langle ij \rangle} t (c_i^\dagger c_j + c_j^\dagger c_i) \quad (4)$$

where  $\epsilon_i$ 's are the site energies and  $t$  is the nearest-neighbor hopping strength. In Eq.(3),  $\Sigma_S$  and  $\Sigma_D$  correspond to the self-energies due to the coupling

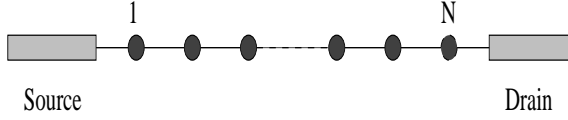


Figure 1: Schematic representation of a bridge system. A one-dimensional conductor with  $N$  atomic sites attached to two metallic electrodes, namely, source and drain.

of the conductor to the source and drain, respectively. All the information regarding the electrode-to-conductor coupling are included into these two self-energies and are described through the use of Newns-Anderson chemisorption theory [20, 21].

The current passing through the conductor can be considered as a single electron scattering process between the two reservoirs of charge carriers. The current-voltage relation can be obtained from the expression [29],

$$I(V) = \frac{e}{\pi\hbar} \int_{-\infty}^{\infty} (f_S - f_D) T(E) dE \quad (5)$$

where the Fermi distribution function  $f_{S(D)} = f(E - \mu_{S(D)})$  with the electrochemical potentials  $\mu_{S(D)} = E_F \pm eV/2$ . Here we assume, for the sake of simplicity, that the entire voltage is dropped across the conductor-to-electrode interfaces and this assumption does not greatly affect the qualitative features of the current-voltage characteristics.

The noise power of the current fluctuations is calculated from the following expression [8],

$$S = \frac{2e^2}{\pi\hbar} \int_{-\infty}^{\infty} [T(E) \{f_S(1 - f_S) + f_D(1 - f_D)\}]$$

$$+ T(E) \{1 - T(E)\} (f_S - f_D)^2] dE \quad (6)$$

where the first two terms of this equation correspond to the equilibrium noise contribution and the last term gives the non-equilibrium or shot noise contribution to the power spectrum. Calculating the noise power we can compute the Fano factor  $F$ , which is essential to predict whether the shot noise lies in the Poisson or the sub-Poisson limit, through the relation [8],

$$F = \frac{S}{2eI} \quad (7)$$

For  $F = 1$ , the shot noise achieves the Poisson limit where no electron correlation exists between the charge carriers. On the other hand for  $F < 1$ , the shot noise reaches the sub-Poisson limit and it provides the information about the electron correlation among the charge carriers.

In this article we focus our results for a moebius strip at very low temperature (5 K), but the qualitative features of all the results are invariant up to some finite temperature ( $\sim 300$  K). For simplicity we take the unit  $c = e = \hbar = 1$  in our all calculations.

### 3 Results and their interpretation

The schematic geometry of a moebius strip is shown in Fig. 2. The two metallic electrodes are attached to the strip at the points  $a$  and  $b$  (colored spots in

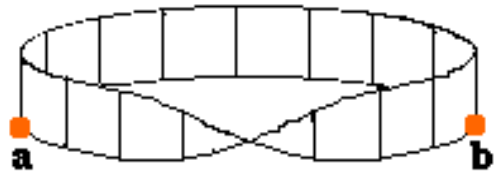


Figure 2: Schematic view of a moebius strip. The two electrodes are attached to the strip at the points  $a$  and  $b$  (colored spots), respectively.

Fig. 2), respectively. In experimental set up, these electrodes are constructed from the gold (Au) atoms and the bridging system is attached to the electrodes by thiol (S-H) groups in the chemisorption technique where the hydrogen (H) atoms remove and the sulfur (S) atoms reside. The tight-binding

Hamiltonian that describes the moebius strip with  $M$  rungs is written in this form,

$$H_C = \sum_{i=1}^{2M} \epsilon_i c_i^\dagger c_i + t \sum_{i=1}^{2M} (c_i^\dagger c_{i+1} + c_{i+1}^\dagger c_i) + t_\perp \sum_{i=1}^{2M} c_i^\dagger c_{i+M} \quad (8)$$

where  $t_\perp$  corresponds to the transverse hopping strength between the two channels,  $t$  represents the nearest-neighbor hopping strength along the longitudinal direction and all the other symbols

We shall describe the electron transport characteristics through the moebius strip in the two different regimes depending on both (a) the transverse hopping strength between the two channels and (b) the coupling strength of the strip to the electrodes. For the transverse hopping strength, we take the two distinct regimes in the following way. One is the case where the electrons are able to hop between the two channels i.e.,  $t_\perp \neq 0$ . Here we take the value of  $t_\perp$  as identical with the value of  $t$ , for simplicity. In the other case the electrons can not move along the transverse direction i.e.,  $t_\perp = 0$ .

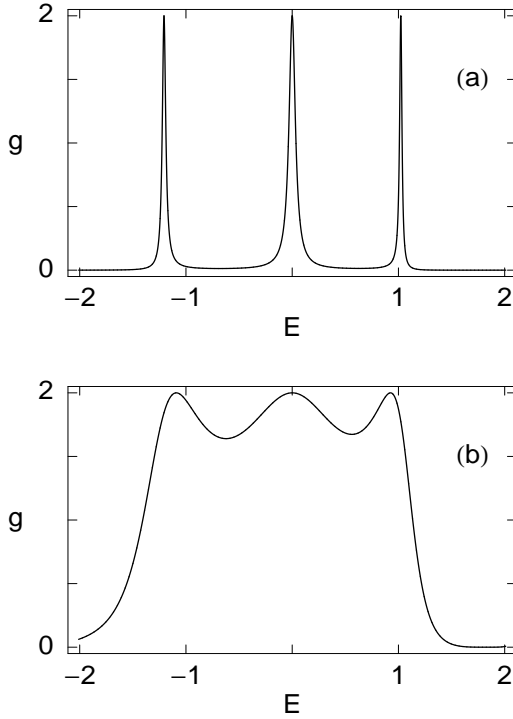


Figure 3: Conductance ( $g$ ) as a function of the injecting electron energy ( $E$ ) for the moebius strip with  $t_\perp \neq 0$ . For this case the strip can be treated as a regular two-channel ring. Here we take the total number of rungs  $M = 6$  (even). (a) and (b) correspond to the results for the weak and the strong coupling limits, respectively.

carry the same meaning as in Eq. 4. This strip has a special kind of geometry and the electron transport is strongly affected by the transverse hopping strength ( $t_\perp$ ). Not only that, the transport characteristics are also significantly influenced by the strip-to-electrode coupling strength ( $\tau_{\{S,D\}}$ ), and, here we focus our results in these two aspects.

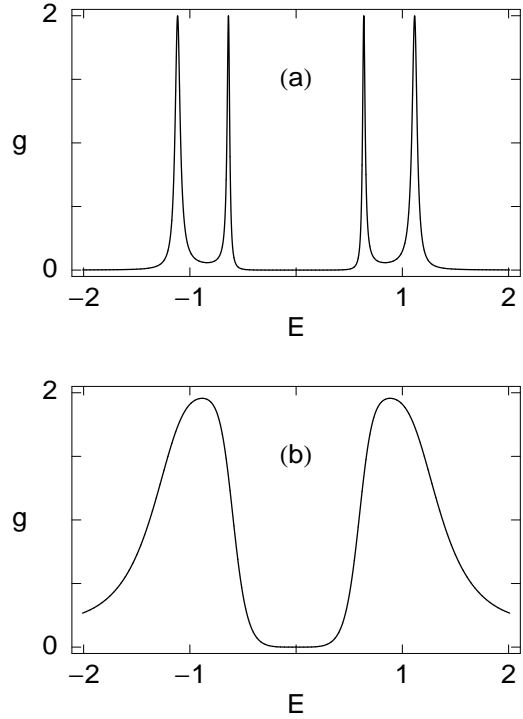


Figure 4: Conductance ( $g$ ) as a function of the injecting electron energy ( $E$ ) for the moebius strip with  $t_\perp = 0$ . For this case the moebius strip reduces to a single chain of length  $2M$ . Here we take  $M = 6$  (even) so that the length of the chain is 12 in unit of the lattice spacing. (a) and (b) correspond to the results for the weak and the strong coupling limits, respectively.

The values of the parameters for these two separate cases are taken as:  $t = t_\perp = 2.5$  and  $t = 2.5, t_\perp = 0$ , respectively. On the other hand depending on the strip-to-electrode coupling strength we classify the two distinct regimes as follows. One is the so-called weak-coupling regime  $\tau_{S(D)} \ll t$  and the other one is the strong-coupling regime  $\tau_{S(D)} \sim t$ , where  $\tau_S$

and  $\tau_D$  are the hopping strengths of the strip to the source and drain, respectively. In our calculations, the parameters in these two regimes are chosen as  $\tau_S = \tau_D = 0.5$ ,  $t = 2.5$  (weak-coupling) and  $\tau_S = \tau_D = 2$ ,  $t = 2.5$  (strong-coupling). Here we set the site energy  $\epsilon_i = 0$  for all the sites of the strip.

In Fig. 3, we plot the conductance  $g$  as a function of the injecting electron energy  $E$  for the moebius strip when the electrons are allowed to hop along

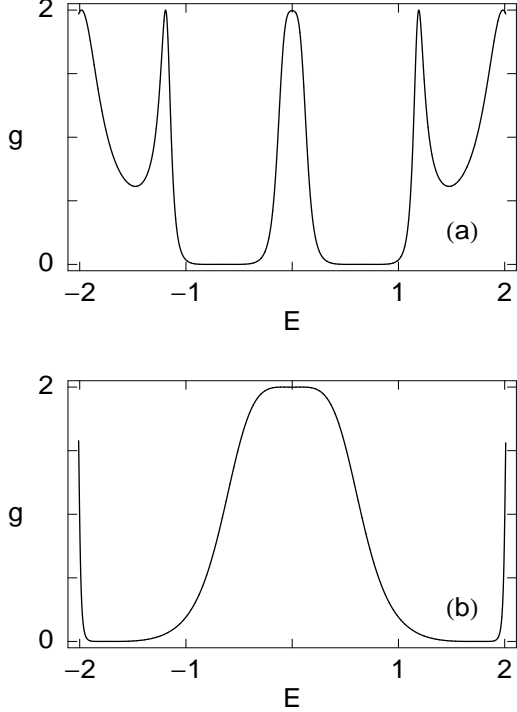


Figure 5: Conductance ( $g$ ) as a function of the injecting electron energy ( $E$ ) for the moebius strip with  $t_{\perp} \neq 0$ . For this case the strip can be treated as a regular two-channel ring. Here we take the total number of rungs  $M = 7$  (odd). (a) and (b) correspond to the results for the weak and the strong coupling limits, respectively.

the transverse direction i.e.,  $t_{\perp} \neq 0$ . For such a case, the moebius strip eventually becomes a small cylinder and no matter it is whether the system is twisted or not. Therefore, for this case the moebius strip can be treated as a regular two-channel ring. Figure 3(a) and (b) correspond to the results of the strip for the weak and the strong coupling limits, respectively. In the limit of weak coupling, the conductance shows sharp resonant peaks (Fig. 3(a)) for some specific energy values, while, for all other energies it drops to zero. At these resonances, the

conductance gets the value 2 and accordingly, the transmission probability  $T$  goes to unity (since from the Landauer conductance formula we get the relation  $g = 2T$  (Eq. 1) as  $e = h = 1$  in our present calculations). These resonant peaks are associated with the energy eigenvalues of the moebius strip.

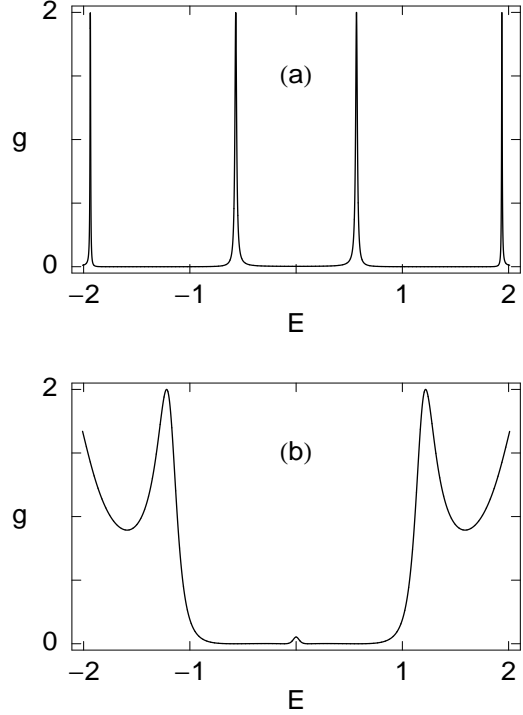


Figure 6: Conductance ( $g$ ) as a function of the injecting electron energy ( $E$ ) for the moebius strip with  $t_{\perp} = 0$ . For this case the moebius strip reduces to a single chain of length  $2M$ . Here we take  $M = 7$  (odd) so that the length of the chain is 14 in unit of the lattice spacing. (a) and (b) correspond to the results for the weak and the strong coupling limits, respectively.

Therefore the conductance spectrum manifests itself the energy eigenvalues of the strip. Now for the strong coupling limit, the widths of these resonant peaks get substantial broadening as observed from Fig. 3(b). This feature appears due to the fact that the energy levels of the strip become broadened in the limit of strong coupling. The contribution for this broadening of the energy levels comes from the imaginary parts of the two self energies  $\Sigma_S$  and  $\Sigma_D$  [29]. From the results shown in Figs. 3(a) and (b), we see that in the weak coupling limit the conduction of the electron through the bridge system takes place for very sharp energy ranges, while, in

the limit of strong coupling the conduction takes place almost for all energy ranges. Therefore, by tuning the coupling strength the electron conduction through the strip can be controlled efficiently.

Figure 4 shows the conductance variation as a function of the energy  $E$  for the moebius strip when the electrons are unable to hop along the transverse direction i.e.,  $t_{\perp} = 0$ . For this particular case ( $t_{\perp} = 0$ ), an electron that moves along the longitudinal direction of the loop encircles the loop twice before returning its starting point. Accordingly, it

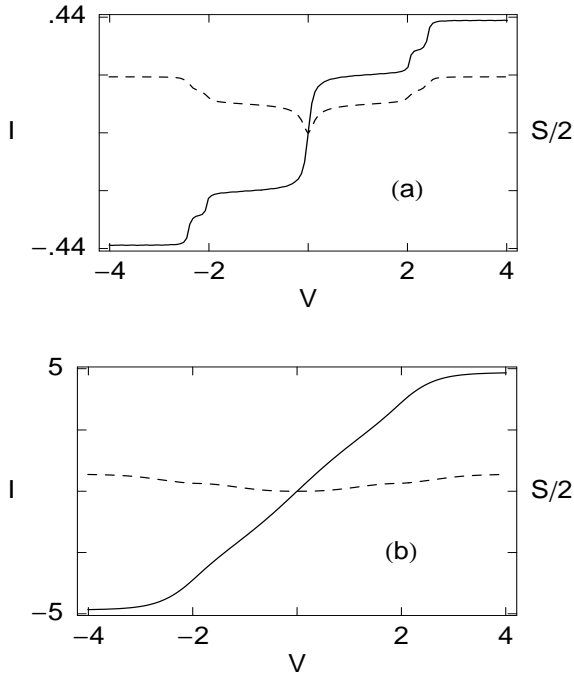


Figure 7: Current  $I$  (solid line) and the noise power of its fluctuations  $S$  (dotted line) as a function of the voltage  $V$  for the moebius strip with  $t_{\perp} \neq 0$ . For this case the moebius strip is equivalent to a two-channel ring. Here we set the total number of rungs  $M = 6$  (even). (a) and (b) correspond to the results for the weak and the strong coupling limits, respectively.

traverses twice path length i.e., the effective length becomes  $2M$  and then the system is treated as a single chain. Here we set  $M = 6$ , to compare the results with the two-channel ring (plotted in Fig. 3), so that the length of the chain becomes  $12$  ( $2M$ ) in unit of the lattice spacing. The results for the weak and the strong coupling limits are given in Figs. 4(a) and (b), respectively. Similar to the results as plotted in Fig. 3, here we also get the sharp resonant

peaks in the conductance spectrum for the weak coupling case, while, these resonances get broadened in the limit of strong coupling. The significant observation is that in this bridge system, both for the weak and strong coupling limits, electron conduction starts beyond some finite value of the energy  $E$  (contrary to the results as given for the moebius strip with finite transverse hopping (Fig. 3), where a sharp resonant peak is observed across the energy  $E = 0$ ). Therefore, the results for the moebius strip with  $t_{\perp} = 0$  (Fig. 4) predict that the electron conducts through the system beyond some critical value of the applied bias voltage.

In order to reveal the dependence of the conductance behavior on the total number of rungs  $M$ , now we describe the results for the moebius strip with odd number of rungs. As illustrative example, in Fig. 5 we plot the conductance  $g$  as a function of the injecting electron energy  $E$  for the moebius strip with non-zero transverse hopping strength i.e.,  $t_{\perp} \neq 0$ . Here we set the total number of rungs  $M = 7$ . The results for the weak and the strong coupling cases are shown in Figs. 5(a) and (b), respectively. Similar to the results observed in Fig. 3, here we also see that the widths of the resonant peaks get broadened as the coupling strength goes from the weak (Fig. 5(a)) to the strong (Fig. 5(b)) limit. Both for the weak and strong coupling cases, we get a sharp resonant peak across the energy  $E = 0$  (similar to the results as described in Fig. 3).

In Fig. 6, we plot the characteristic behavior of the conductance  $g$  as a function of the energy  $E$  for the moebius strip ( $M = 7$ ) when the electrons are unable ( $t_{\perp} = 0$ ) to hop along the transverse direction. Figure 6(a) and (b) correspond to the results for the weak and strong coupling cases, respectively. These features are almost quite similar to the results predicted for the moebius strip with even ( $M = 6$ ) number of rungs considering  $t_{\perp} = 0$  (see Fig. 4). From the results given in Fig. 6, we see that the electron starts conduction across the strip beyond some finite value of the energy  $E$ , similar to the results as observed in Fig. 4. Thus we can emphasize that the threshold bias voltage of the electron conduction through the moebius strip can be controlled very significantly by tuning the transverse hopping strength ( $t_{\perp}$ ). From the results studied above we see that the behavior of the electron conduction is highly influenced by the peculiar topology of the moebius strip.

The behavior of the electron conduction through the moebius strip is much more clearly visible by studying the current-voltage ( $I$ - $V$ ) characteristics.



In the forthcoming part we shall discuss the characteristics of the current ( $I$ ) and the noise power of its fluctuations ( $S$ ) as a function of the applied bias voltage ( $V$ ). Both the current ( $I$ ) and the noise power of its fluctuations ( $S$ ) are computed by the integration procedure of the transmission function  $T$ , as given in Eq.(5) and Eq.(6), respectively. The variation of the transmission function  $T$  is similar to that of the conductance spectra, differ only in magnitude by a factor 2 (since  $g = 2T$ , from the Landauer conductance formula), as shown in Figs. 3, 4, 5 and 6.

In Fig. 7, we draw the current and the noise power of its fluctuations as a function of the bias voltage for the moebius strip in the limit of non-zero transverse hopping strength ( $t_{\perp} \neq 0$ ). Here we set the total number of rungs  $M = 6$ , same as in the study of Fig. 3. In this case ( $t_{\perp} \neq 0$ ) the moebius strip is equivalent to a regular two-channel ring since the electrons can able to move along the transverse direction. Figure 7(a) and (b) correspond to the weak and the strong coupling cases, respectively, where the solid curves correspond to the current and the dotted curves represent the noise power. For the weak coupling limit, the current shows staircase-like behavior with sharp steps (solid curve of Fig. 7(a)) associated with the sharp resonant peaks in the conductance spectrum (Fig. 3(a)), since the current is evaluated by the integration procedure of the transmission function  $T$ . On the other hand, as the coupling strength increases the staircase-like behavior disappears and the current varies continuously with the applied voltage  $V$ , as shown by the solid curve in Fig. 7(b). This is due to the broadening of the resonant peaks in the conductance spectrum (Fig. 3(b)) for the limit of strong coupling. The another important point is that with the increase of the coupling strength, the current amplitude gets an order of magnitude enhancement which is clearly observed by comparing the results given by the solid curves in Figs. 7(a) and (b). This feature can be understood by noting the areas under the curves those are plotted in Figs. 3(a) and (b), respectively. Both for the weak and strong coupling cases, we get finite value of the current momentarily as we switch on the bias voltage across this bridge. Now in the determination of the noise power of the current fluctuations (dotted curves in Fig. 7), we see that both for the two coupling cases the shot noise achieves the sub-Poisson limit ( $F < 1$ ). Therefore, we can predict that the electrons are correlated with each other. Here the electrons are correlated only in the sense that one electron feels the existence of the other ac-

cording to the Pauli exclusion principle (since we have neglected all other types of electron-electron interactions in our present formalism).

The characteristic properties of the current and the noise power of its fluctuations are much more interesting for the case where the electrons are unable to hop along the transverse direction i.e.,  $t_{\perp} = 0$ . For this particular case ( $t_{\perp} = 0$ ), as we have men-

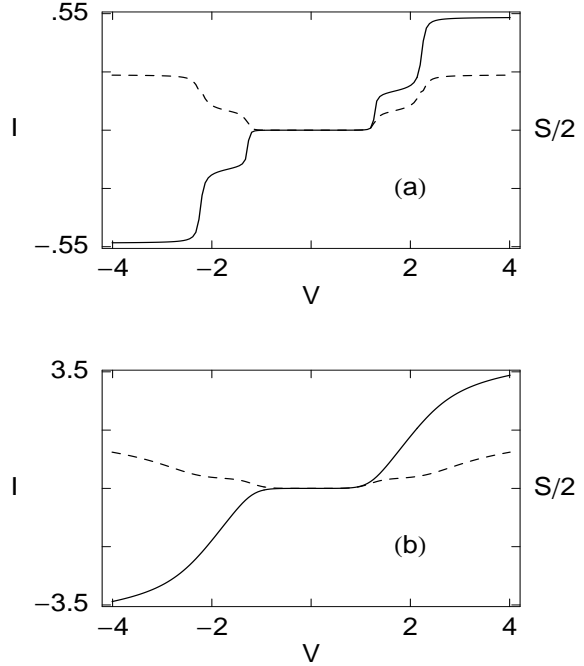


Figure 8: Current  $I$  (solid line) and the noise power of its fluctuations  $S$  (dotted line) as a function of the voltage  $V$  for the moebius strip with  $t_{\perp} = 0$ . For this particular case the moebius strip is equivalent to a single chain of length  $2M$ . Here we take  $M = 6$  (even) so that the length of the chain becomes 12 in unit of the lattice spacing. (a) and (b) correspond to the results for the weak and the strong coupling limits, respectively.

tioned earlier, the moebius strip eventually reduces to a single chain with length  $2M$ . This is due to the strange topological behavior of the moebius strip. Figure 8 shows the results for the moebius strip when  $t_{\perp} = 0$ , where Figs. 8(a) and (b) correspond to the results for the weak and strong coupling cases, respectively. Here we take  $M = 6$ , so that the length of the chain becomes 12, same as in the study of the conductance behavior (plotted in Fig. 4). The solid and dotted curves of Fig. 8 represent the same meaning as in Fig. 7. For the

weak coupling limit, the current shows staircase-like behavior (solid curve of Fig. 8(a)), while, it gets a continuous variation (solid curve of Fig. 8(b)) in the limit of strong coupling as a function of the applied bias voltage, similar to the results as predicted for the strip with  $t_{\perp} \neq 0$  (solid curves of Figs. 7(a) and (b), respectively). The significant observation is that for this bridge (strip with  $t_{\perp} = 0$ ), both for the weak and strong coupling limits, the current appears after some critical value of the applied bias voltage (contrary to the results as given for the bridge with  $t_{\perp} \neq 0$  i.e., for a regular two-channel ring (Fig. 7)). Thus the electron transport through the moebius strip can be tuned significantly by controlling the transverse hopping strength. A similar kind of behavior has also been observed in the conductance spectra for the moebius strip with  $t_{\perp} \neq 0$  and  $t_{\perp} = 0$  cases, respectively. Finally, in the study of the noise power of the current fluctuations for this bridge we see that both for the two coupling cases the shot noise goes from the Poisson limit ( $F = 1$ ) to the sub-Poisson limit ( $F < 1$ ) as long as we cross the first step in the current-voltage characteristics. Therefore, we can predict that the electrons are correlated after the tunneling process has completed in this bridge. This result is different from our previous studies i.e., the result for the strip with  $t_{\perp} \neq 0$  where the shot noise always lies in the sub-Poisson limit and there is no such possibility of transition from the Poisson limit to the sub-Poisson limit.

For the moebius strip with odd number of rungs we get quite similar features, as described above, in the current-voltage characteristics and also in the noise power of the current fluctuations. This is why here we do not describe these features further for the moebius strip with odd number of rungs.

## 4 Concluding remarks

To summarize, we have introduced a parametric approach based on the tight-binding model to investigate the electron transport properties through a moebius strip attached to two metallic electrodes. The topological effect of the moebius strip has an important signature in the electron transport through such system. For the case where electrons are able to hop along the transverse direction, the moebius strip becomes a regular two-channel ring. On the other hand, if the electrons are unable to hop along the transverse direction then the system reduces to a single chain with doubling its length than the previous one. Here we have described our results both for these two cases and obtained several

interesting results.

For the weak-coupling limit, the conductance shows sharp resonant peaks (Figs. 3(a), 4(a), 5(a) and 6(a)) associated with the energy eigenvalues of the moebius strips. The widths of these resonant peaks become broadened substantially (Figs. 3(b), 4(b), 5(b) and 6(b)) in the limit of strong coupling, where the contribution comes from the imaginary parts of the two self-energies,  $\Sigma_S$  and  $\Sigma_D$ , due to coupling of the strip to the electrodes [29]. Both for the moebius strips with odd and even number of rungs, the threshold bias voltage of the electron conduction can be tuned very nicely by controlling the transverse hopping strength  $t_{\perp}$  which provides an important finding.

In the study of  $I$ - $V$  characteristics we have seen that the current shows staircase-like behavior with sharp steps (solid curves of Figs. 7(a) and 8(a)) in the weak-coupling limit, while it varies continuously and achieves higher amplitude (solid curves of Figs. 7(b) and 8(b)) with the increase of the coupling strength.

In the determination of the noise power of the current fluctuations, we have noticed that for the strip with  $t_{\perp} \neq 0$  the shot noise lies always in the sub-Poisson limit ( $F < 1$ ) (dotted curves of Fig. 7) i.e., the electrons are correlated with each other. On the other hand for the strip with  $t_{\perp} = 0$  the shot noise makes a transition from the Poisson limit ( $F = 0$ ) to the sub-Poisson limit ( $F < 1$ ) after the first step in the  $I$ - $V$  curve (dotted curves of Fig. 8).

Throughout our discussions we have used several approximations by neglecting the effects of the electron-electron interaction, all the inelastic processes, the Schottky effect, the static Stark effect, etc. More studies are expected to take into account all these approximations for our further investigations.

## References

- [1] A. Aviram and M. Ratner, Chem. Phys. Lett. **29**, 277 (1974).
- [2] R. M. Metzger *et al.*, J. Am. Chem. Soc. **119**, 10455 (1997).
- [3] C. M. Fischer, M. Burghard, S. Roth, and K. V. Klitzing, Appl. Phys. Lett. **66**, 3331 (1995).
- [4] J. Chen, M. A. Reed, A. M. Rawlett, and J. M. Tour, Science **286**, 1550 (1999).
- [5] M. A. Reed, C. Zhou, C. J. Muller, T. P. Burgin, and J. M. Tour, Science **278**, 252 (1997).



- [6] T. Dadosh, Y. Gordin, R. Krahne, I. Khivrich, D. Mahalu, V. Frydman, J. Sperling, A. Yacoby, and I. Bar-Joseph, *Nature* **436**, 677 (2005).
- [7] Y. Xue and M. A. Ratner, *Phys. Rev. B* **68**, 115407 (2003).
- [8] Y. M. Blanter and M. Büttiker, *Phys. Rep.* **336**, 1 (2000).
- [9] S. Tanda, T. Tsuneta, Y. Okajima, K. Inagaki, K. Yamaya, and N. Hatakenaka, *Nature* **417**, 397 (2002).
- [10] K. Yakubo, Y. Avishai and D. Cohen, *Phys. Rev. B* **67**, 125319 (2003).
- [11] E. H. M. Ferreira, M. C. Nemes, M. D. Sampaio and H. A. Weidenmüller, *Phys. Lett. A* **333**, 146 (2004).
- [12] S. N. Yaliraki, A. E. Roitberg, C. Gonzalez, V. Mujica, and M. A. Ratner, *J. Chem. Phys.* **111**, 6997 (1999).
- [13] M. Di Ventra, S. T. Pantelides, and N. D. Lang, *Phys. Rev. Lett.* **84**, 979 (2000).
- [14] Y. Xue, S. Datta, and M. A. Ratner, *J. Chem. Phys.* **115**, 4292 (2001).
- [15] J. Taylor, H. Gou, and J. Wang, *Phys. Rev. B* **63**, 245407 (2001).
- [16] P. A. Derosa and J. M. Seminario, *J. Phys. Chem. B* **105**, 471 (2001).
- [17] P. S. Damle, A. W. Ghosh, and S. Datta, *Phys. Rev. B* **64**, R201403 (2001).
- [18] M. Brandbyge, J. -L. Mozos, P. Ordejon, J. Taylor, and K. Stokbro, *Phys. Rev. B* **65**, 165401 (2002).
- [19] A. R. Rocha, V. M. Garcia-Suarez, S. Bailey, C. Lambert, J. Ferrer, and S. Sanvito, *Phys. Rev. B* **73**, 085414 (2006).
- [20] V. Mujica, M. Kemp, and M. A. Ratner, *J. Chem. Phys.* **101**, 6849 (1994).
- [21] V. Mujica, M. Kemp, A. E. Roitberg, and M. A. Ratner, *J. Chem. Phys.* **104**, 7296 (1996).
- [22] M. P. Samanta, W. Tian, S. Datta, J. I. Henderson, and C. P. Kubiak, *Phys. Rev. B* **53**, R7626 (1996).
- [23] M. Hjort, S. Stafström, *Phys. Rev. B* **62**, 5245 (2000).
- [24] R. Baer and D. Neuhauser, *Chem. Phys.* **281**, 353 (2002).
- [25] R. Baer and D. Neuhauser, *J. Am. Chem. Soc.* **124**, 4200 (2002).
- [26] D. Walter, D. Neuhauser and R. Baer, *Chem. Phys.* **299**, 139 (2004).
- [27] K. Walczak, *Cent. Eur. J. Chem.* **2**, 524 (2004).
- [28] K. Walczak, *Phys. Stat. Sol. (b)* **241**, 2555 (2004).
- [29] S. Datta, *Electronic transport in mesoscopic systems*, Cambridge University Press, Cambridge (1997).